

Life-history traits of alvinocaridid shrimps inhabiting chemosynthetic ecosystems around Japan

Authors and Affiliations

Pierre Methou¹, Verity Nye², Jonathan T. Copley², Hiromi Kayama Watanabe¹, Yukiko Nagai¹, Chong Chen¹

¹X-STAR, Japan Agency for Marine-Earth Science and Technology (JAMSTEC), Yokosuka, 237-0061, Japan

²Ocean and Earth Science, National Oceanography Centre Southampton, University of Southampton, Southampton SO14 3ZH, United Kingdom

Keywords

Crustacean, deep sea, hydrothermal vent, hydrocarbon seep, life cycle, reproduction

Abstract

Alvinocaridid shrimps are endemic and globally widespread in chemosynthetic ecosystems such as hydrothermal vents and hydrocarbon seeps. Though the biology of Atlantic alvinocaridid species have received considerable attention, little is known about their Pacific relatives. Here we described population structures and reproductive biology of three Pacific alvinocaridid species – *Shinkaicaris leurokolos*, *Opaepele loihi*, *Alvinocaris longirostris* – with notes on a fourth species – *A. dissimilis* – from several chemosynthetic ecosystems around Japan and compared their size frequency distributions and reproductive outputs. We showed that population demographics differ among these species, including a significantly larger proportion of juveniles in *O. loihi* and spatial variation of sex ratio in *S. leurokolos*, but all shared sex ratios biased toward females. The three shrimp species were characterized by relatively small sizes at onset of maturity, although this varied among sites for *A. longirostris*. Overall, size-specific fecundities and egg volumes of *A. longirostris*, *O. loihi* and *S. leurokolos* were in a similar range to Atlantic alvinocaridids. In addition, we performed egg incubation experiments of *O. loihi* under different temperature conditions to characterize thermal physiology during its brooding period. This confirmed a strong influence of temperature on both brooding duration and hatching rate, with a thermal preference that differs from previously published data for *A. longirostris* and *S. leurokolos*. Finally, our results indicated that these alvinocaridid species from the northwestern Pacific likely differ in reproductive timing, either through distinct brooding durations and/or distinct brooding periodicity, although further investigations are required to confirm these patterns.

Introduction

Deep-sea chemosynthetic ecosystems fueled by geofluids, such as hydrothermal vents and hydrocarbon seeps, constitute lush and isolated hotspots of high biomass and endemism,

but relatively low faunal diversity compared with other deep-sea habitats (Van Dover and Trask 2000). These environments are typically unstable and ephemeral, particularly hydrothermal vents where fluid activity at a given location is intermittent and can often cease within decadal timescales (Van Dover 2019). The persistence of endemic species over successive generations is greatly interlinked with their ability to disperse and colonize these dynamic and patchy habitats (Vrijenhoek 2010; Mullineaux et al. 2018). Like most marine invertebrates (Cowen and Sponaugle 2009), many specialized fauna from vents and seeps exhibit a biphasic lifecycle with a larval phase connecting the different benthic populations. Demographic structures of populations at a given site thereby result from the number of competent larvae reaching and settling there – depending on the likelihood of a successful settlement – and any mortality events occurring between successive life stages (Kelly and Metaxas 2007). Consequently, any environmental factors or life-history traits affecting one of these steps have implications on population sizes and connectivity between populations. A thorough knowledge of biological traits governing the demography and connectivity of vent and seep endemic species is not only essential for understanding the mechanisms shaping their biogeography but also for drafting efficient conservation strategies (Van Dover et al. 2018; Danovaro et al. 2020; Gollner et al. 2021), within a context of imminent deep-sea mining scheduled to take place within the next few years (Miller et al. 2018).

Widely distributed in vents and seeps across the globe, shrimps in the family Alvinocarididae are restricted to chemosynthesis-based ecosystems (Lunina and Vereshchaka 2014; Zbinden and Cambon-Bonavita 2020), often dominating faunal assemblages (Nye et al. 2013; Hernández-Ávila et al. 2022; Methou et al. 2022a). In most studied cases, these species exhibit high connectivity across large distances along mid-oceanic ridges (Teixeira et al. 2012, 2013; Beedessee et al. 2013; Zhou et al. 2022) or between back-arc basins (Thaler et al. 2014; Yahagi et al. 2015) indicating possible high realized dispersal potentials. In characterizing life-history traits linked to dispersal capability, observations of first zoea stages in four alvinocaridid species have revealed an atypical combination of morphological characteristics suggesting an early lecithotrophic phase with an extended larval development (Hernández-Ávila et al. 2015). This early lecithotrophy is followed by a planktotrophic phase in the late larvae, as indicated by their carbon and sulfur isotopic ratios as well as the composition of the lipid storages in their juveniles that differed from the typical chemosynthetic signature found in adults (Pond et al. 1997; Stevens et al. 2008; Methou et al. 2020). Whether these larvae are transported by currents in bottom water, mid-water, or surface water during their dispersal phase remains contested (Methou et al. 2020). As for most decapods, alvinocaridid shrimps maintain eggs below their abdomen but a variety of brooding cycles can be seen the family, including seasonal patterns in some species and aperiodic brooding along the year in others like *Mirocaris fortunata* (Ramirez-Llodra et al. 2000; Methou 2019). Among the seasonal breeders, some shrimps' reproduction cycles follow variations of sinking photosynthetic particles, such as *Alvinocaris stactophila* from the Gulf of Mexico (Copley and Young 2006). Conversely, reproductive cycles of *R. exoculata* and *R. kairei* from the Atlantic and Indian oceans revealed a more unusual periodicity, restricted between January and early April in both the northern and the southern hemispheres, and thus unlinked to surface production (Methou et al. 2022b).

Similar to other chemosynthetic endemic groups such as *Bathymodiulus* mussels (Husson et al. 2017) and *Kiwa* 'yeti crabs' (Marsh et al. 2015), alvinocaridid shrimps also display

complex demographic patterns with small-scale spatial segregation between their different benthic life stages. This includes distinct nurseries habitats for early juvenile conspecifics of alvinocaridids at Atlantic hydrothermal vents, which occupy cooler thermal niches than their adult stages (Hernández-Ávila et al. 2022; Methou et al. 2022a). Brooding females, on the other hand, have been observed both within adult aggregations in close vicinity to the hot vent fluid emissions for *R. exoculata*, *R. kairei*, and *R. hybisae* (Nye et al. 2013; Methou et al. 2022b, a), or preferentially at the center of the brine pool seep site for *A. stactophila*, less exposed to stronger hypoxic and sulfidic conditions from the peripheral fluid emission zones (Copley and Young 2006). However, most of our knowledge is based on Atlantic species and significant gaps remain about the lifecycle ecology of alvinocaridids from other regions.

In the Northwest Pacific, five alvinocaridids species have been reported in different chemosynthetic ecosystems around Japan: *Shinkaicaris leurokolos* and *A. dissimilis* in the Okinawa Trough, *Opaepele loihi* in the Izu-Bonin-Mariana (IBM) Arcs, and *Alvinocaris longirostris* and *Alvinocaris marimonte* across both regions (Nakajima et al. 2014; Watanabe et al. 2019; Brunner et al. 2022). Additionally, *A. longirostris* also inhabits hydrocarbon seeps in Sagami Bay and South China Sea (Li 2015; Yahagi et al. 2015; Ke et al. 2022). Populations of these species differed in their genetic structure, with a greater genetic diversity in *S. leurokolos* compared to the other species, but also in their small-scale distribution at hydrothermal vent sites, with a segregation between *A. longirostris* in cooler areas and *S. leurokolos* closer to hot fluid emissions (Yahagi et al. 2015). Hatching incubation experiments with egg masses under different temperature conditions also revealed similar thermal preferences for brooding and larval stages in these two species (Watanabe et al. 2016).

Here, we investigated demographic structures and reproductive biology of three of these alvinocaridid species inhabiting hydrothermal vent and hydrocarbon seep sites – *S. leurokolos*, *O. loihi*, *A. longirostris* – with notes on a fourth one, *A. dissimilis*, by comparing their size-frequency distributions and their reproductive outputs determined as fecundities and egg volumes. Our study addresses the following questions: (1) what are the reproductive traits, such as size-specific fecundities and egg volumes, of alvinocaridids from the Northwest Pacific? (2) Is there significant variation in population structures and reproductive traits of alvinocaridid among distinct sampling sites or among distinct assemblages from the same sampling site? (3) Does reproductive traits and population structures of Northwest Pacific alvinocaridids differ from vent shrimps inhabiting other regions? Additionally, we performed incubation experiments of *O. loihi* egg broods under different thermal conditions to compare with our previous study of alvinocaridid species from the same region (Watanabe et al. 2016).

Materials and Methods

Field sampling

Alvinocaridid shrimps were collected between 2005 and 2022 during eight cruises surveying hydrothermal vents in the Okinawa Trough (Sep 2010, Jan 2014, Jul-Aug 2015, Oct 2015, Nov 2015, Nov-Dec 2016 and Aug 2017), six cruises to vents on the Izu-Ogasawara Arc and the Off Hatsushima seep in Sagami Bay (Aug 2019, Mar 2022, Feb 2021, Sept 2021, May-Jun

2022 and Feb 2022) and one cruise on the Ryukyu Arc (May 2005). For detailed information of sampling localities, see Fig. 1 and Table S1. In total, 22 spatially discrete samples of shrimps were collected from seven vent fields in the Okinawa Trough as well as three samples from two vent fields on the Izu-Ogasawara Arc, three samples from the Off Hatsushima hydrocarbon seep within the Sagami Bay and one sample from the Kuroshima Knoll methane seep on the Ryukyu Arc (Fig. 1).

Shrimps were taken from faunal assemblages using suction samplers mounted on the Remotely Operated Vehicles (ROV) *Kaiko*, *Hyper-Dolphin*, or *KM-ROV* or the Human Operated Vehicle (HOV) *Shinkai 6500*. At the Suiyo Seamount, temperature of the assemblages where the shrimps were collected were measured using a RINKO stand-alone dissolved oxygen/temperature probe (RINKO I, JFE Advantech, Japan) for three minutes. Upon recovery on-board the research vessels, specimens were sorted by species from the rest of the vent fauna and stored in either 99% EtOH or 10% buffered formalin.

Identifications and measurements of shrimps

For each shrimp, the carapace length (CL) was measured with a vernier caliper from the posterior margin of the eye orbit to the posterior margin of the carapace, with an estimated precision of 0.1 mm. Each individual was identified and sorted by sex according to the shape of the endopod of the first pleopod and the occurrence of the appendix masculina on the second pleopod in males (Komai and Segonzac 2005). Since juveniles (i.e. immature individuals) could not be distinguished morphologically from mature females, individuals with a CL smaller than the smallest recorded male of each species (Table 1) were categorized as juveniles in our analyses.

Shrimp species from newly collected localities with no published records (Higashi-Aogashima, Suiyo Seamount, and Kuroshima Knoll) and small *Alvinocaris* juveniles were subjected to DNA barcoding to confirm their identity. Genomic DNA was extracted from pieces of muscle with the DNeasy Blood & Tissue kit (Qiagen) following the manufacturer's instructions. To avoid amplification of potential mitochondrial pseudogenes, Cari-COI-1F and Cari-COI-1R primers, specifically designed for alvinocaridids, were used (Methou et al. 2020). Amplification was performed in 25 µl reaction mixture containing 10.5 µl of RNase free H₂O, 12.5 µl of 2× Premix ExTaq HS buffer (TaKaRa Bio Inc.) containing the dNTP mix and Ex Taq DNA polymerase, 0.5 µl of each primer at 10 µM, and 1 µL of shrimp's DNA. Thermal cycling parameters used an initial denaturation at 95 °C for 5 min, followed by 35 cycles at 95 °C for 1 min, 50°C for 1min, 72 °C for 2min and a final 10 min extension cycle at 72°C. Amplicons were sequenced by Sanger sequencing on both strands by FASMAC Corporation (Kanagawa, Japan). To check the species identity, each individual sequence was blasted against the NCBI database.

Identification of reproductive status and measurements of eggs

Reproductive status of females was defined in non-ovigerous and ovigerous females following published methods (Nye et al. 2013), with ovigerous females including both brooding females bearing egg broods under their abdomen and hatched females that have recently

released their larvae but still retained modified pleopods, indicative of a recent brooding status. For each brooding female, the total number of eggs was manually counted and thirty eggs per brood were randomly selected to measure the egg diameters. Volumes of eggs was estimated following a published method (Hernández-Ávila et al. 2022), considering a spheroid volume $v = \frac{4}{3}\pi \cdot r_1 \cdot r_2^2$, where r_1 and r_2 are half of maximum and minimum axis of each egg respectively. Embryonic and post-embryonic stages, seen through the transparent envelope of eggs, were classified in three developmental stages (early, mid, late) according to Methou et al. (2022b). Females with hatched or damaged broods were not included in our reproductive analyses (egg number, egg volumes, and egg stages).

Culture experiment of *O. loihi* egg broods under different temperature conditions

Among 103 ovigerous females of *Opaepele loihi* collected from Suiyo Seamount in August 2019, ten individuals were still alive following recovery on-board and kept in a cold-water tank at 4°C. All parent shrimps died within 16 days after the collection event. All eggs were removed from the female pleopods and transferred to 10 mL of cold (4 °C), 0.22 µm filtered seawater. The eggs were separated in several batches (up to 5) comprised of 18 to 20 eggs brooded by the same individual, and placed in a series of incubators with temperatures set to 5°C, 10°C, 15°C, 20°C, and 25°C, to examine temperature effect to the survival and hatching rates of the eggs. Among the ten egg masses, only three hatched under our rearing conditions to enable comparison of development under different brooding temperatures.

Each batch of eggs was kept in a 13.5 mL glass bottle, washed three times with filtered seawater (pore size = 0.2 µm) and filled with 10 mL of filtered seawater, half of which was exchanged every two to three days (three times per week). Conditions of the eggs were observed under a stereo microscope (Olympus SZX7) at each seawater exchange and their survival rates and hatching rates were recorded. As their exoskeleton was transparent and their movement was easy to observe, larval death was assessed when individuals were observed to be unresponsive after stimulation, and when their yolk reserves (yellow to orange in color) were depleted. We considered the larvae as hatched when they were found out of their egg envelopes.

Statistical analysis

Alvinocaridid shrimps were grouped first by species and then either by sex/reproductive status or by sampling localities. Due to sampling limitation and for statistical purposes, only populations with more than 10 individuals per localities per sampling period were included for analyses of size-frequency distribution and with more than 40 individuals for cohort analyses. Similarly, analyses of fecundities, egg volumes, and egg stage proportions could not be performed for *A. dissimilis* due to the limited available sample size of their ovigerous stages.

Visual examination of our dataset and Shapiro-Wilk normality tests revealed that the size (i.e., carapace length: CL), egg number, and egg volumes of alvinocaridids deviated from the normal distribution. Non-parametric tests were therefore used for intergroup comparison with a Mann-Whitney test when two groups were compared, or a Kruskal-Wallis test followed by

post-hoc Dunn tests when three or more groups were compared. Frequencies of males and females in groups were tested for significant variation from a 1:1 sex ratio using a χ^2 test with a Yates correction for 1 df. Relationships between \log_e -transformed realized fecundity and \log_e -transformed carapace length of the different shrimp groups were assessed using Spearman rank-order correlations. Groups with less than five individuals were excluded from statistical analyses. Cohort analyses were realized using the 'mixdist' R package (Macdonald and Du 2012) following the same method used by (Methou et al. 2022a). In brief, size-frequency histograms were plotted with a 1 mm size class interval, following criteria defined by (Jollivet et al. 2000). Modal decompositions, fitted to these histograms, were considered as valid according to the χ^2 test from the 'mixdist' package. Components of the modal decomposition were defined as the proportion (%), the mean CL size (μ) and the standard deviation of the CL size (σ) of a defined cohort. All analyses were performed in R v. 4.1 (R Core Team 2020).

Results

Size-frequency distributions

Population structures of the four alvinocaridid shrimp species from hydrothermal vents and hydrocarbon seeps around Japan clearly differed in several aspects (Fig. 2). Body size variations were observed among populations from distinct sampling years and sites for *S. leurokolos* (Kruskal-Wallis $H = 69.53$, $p < 0.001$; Table 1) as well as for *A. longirostris* (Kruskal-Wallis $H = 166.7$, $p < 0.001$). Specifically, *S. leurokolos* populations from Daisan Kume in 2016 and Gima Knoll in 2015 were significantly smaller than those from other vent fields (Dunn's Multiple Comparison Test, $p < 0.001$) whereas *A. longirostris* from Tarama Knoll in 2015 were significantly smaller than populations from any other sites (Dunn's Multiple Comparison Test, $p < 0.001$). In addition, *A. longirostris* populations from Sakai in July-August 2015 were larger than populations from Futagoyama, Tarama Knoll (both in 2015 and 2017) and Daisan Kume in 2016 (Dunn's Multiple Comparison Test, $p < 0.001$). Variations in size between *A. longirostris* populations from the same site but sampled at different periods were also found both at Tarama Knoll between 2015 and 2017 and at Sakai between July-August 2015 and November 2015 (Dunn's Multiple Comparison Test, $p < 0.001$).

For both *S. leurokolos* and *A. longirostris* (Kruskal-Wallis, *S. leurokolos*: $H = 71.02$, $p < 0.001$; *A. longirostris*: $H = 31.87$, $p < 0.001$) females were significantly larger than males (Dunn's Multiple Comparison Tests, $p < 0.001$). Ovigerous females of *S. leurokolos* were only significantly larger than males (Dunn's Multiple Comparison Test, $p < 0.001$) whereas ovigerous females of *A. longirostris* were significantly larger than both males and non-ovigerous females (Dunn's Multiple Comparison Tests, $p < 0.001$). Despite these sizes variations, the smallest recorded adults were of similar sizes for all species (Table 1), at CL 4.9 mm for *Opaepele loihi*, CL 4.5 mm for *Shinkaicaris leurokolos*, CL 4.8 mm for *Alvinocaris longirostris*, and CL 4.0 mm for *Alvinocaris dissimilis*.

Cohort analyses

The MIX modal decomposition of *O. loihi* from Suiyo revealed two distinct cohorts, with the first cohort including nearly 3/4 of the total population (Table 2 & Fig. S1A). The *S. leurokolos* population from Iheya North in 2014 were composed of three cohorts (Table 2 & Fig. S1B) whereas *A. longirostris* populations from Sakai in 2015 were in two distinct cohorts (Table 2 & Fig. S1C). These populations had limited proportion of individuals in their first cohorts (*S. leurokolos* from Iheya North in 2014: 13.8%; *A. longirostris* from Sakai in Jul-Aug 2015: 6%) or showed equilibrated proportions between the two cohorts. Two populations – *S. leurokolos* from Iheya North in 2013 and *A. longirostris* from Tarama Knoll in 2015 – followed a normal distribution with a single cohort detected by the MIX analysis.

Life stage and sex ratio distributions

Large variations in the proportions of males and females were also observed in the alvinocaridid species (Fig. 2; Table 1). Sex ratio of *O. loihi* from Suiyo was significantly female-biased ($\chi^2 = 22.94$, $p < 0.001$). Samples of *S. leurokolos* were either biased toward females at Iheya North in 2013 and 2014 (2013: $\chi^2 = 51.07$, $p < 0.001$; 2014: $\chi^2 = 55.78$, $p < 0.001$), toward males at Daisan Kume and Gima knolls (Daisan Kume: $\chi^2 = 5$, $p < 0.001$; Gima Knoll: $\chi^2 = 8.33$, $p < 0.001$) or did not deviate significantly from 1:1 at Izena Hole ($\chi^2 = 0$, $p > 0.05$). The sex ratios of *A. longirostris* were clearly female-biased at Sakai and Izena Hole (Sakai: $\chi^2 = 22.51$ and 41.67 , $p < 0.001$; Izena Hole: $\chi^2 = 14.44$, $p < 0.001$), only slightly biased at Daisan Kume in 2015 ($\chi^2 = 4.45$, $p < 0.05$) or exhibited equilibrated proportions of males and females at Daisan Kume in 2016, Tarama Knoll, and Futagoyama ($\chi^2 = 0.5 - 3.9$, $p > 0.05$; see Table 1.).

Moreover, marked spatial variations in sex ratio of *S. leurokolos* could be observed among sampling events from the Iheya North field in February 2014 (Table 3) with two female-biased samples ($\chi^2 = 14.92$ and 62.08 , $p < 0.001$) and two male-biased samples ($\chi^2 = 18$, $p < 0.001$; $\chi^2 = 3.86$, $p < 0.05$). Conversely, most sampling events of *A. longirostris* from Sakai exhibited sex ratio biased toward females ($\chi^2 = 5.44 - 21$, $p < 0.001$; see Table 3) with only one sample in August 2015 that did not deviate significantly from a 1:1 sex ratio ($\chi^2 = 3$, $p > 0.05$). Additionally, the population structure of *O. loihi* exhibited a striking difference from the others in that the juvenile individuals dominated, constituting 71.9% of the sampled population, whereas juveniles were scarce in the other three species – representing at most 29.4% of the Tarama Knoll population of *A. longirostris*.

The alvinocaridid species differed also in the types of colonized faunal assemblages (Fig. 3 and Table S1). While *Shinkaicaris leurokolos* were restricted to chimney surfaces near active venting or in close vicinity of *Shinkaia crosnieri* squat lobsters (Fig. 3A) in Okinawa Trough vents, *A. longirostris* were found in all types of assemblage sampled, including chimney surfaces (Fig. 3B), tubeworm bushes (Fig. 3D and F), mussel beds (Fig. 3E), and sponge colonies (Fig. 3G). Both *O. loihi* and *A. dissimilis* were restricted to a single assemblage type: mussel beds for *O. loihi* and sponge colonies for *A. dissimilis*, although their sampling was more limited, as they were only collected during one and three sampling events respectively.

Reproductive stage proportions

Our samples provide some information for understanding the reproductive seasonality (or the lack of it) in the four species examined. A large number of *Opaepele loihi* ovigerous females was collected in August 2019 at Suiyo, with 103 ovigerous individuals representing 43.8% of all the females collected at this vent field (Fig. 2A). Similarly, substantial numbers of *S. leurokolos* ovigerous females were collected in November 2013 and February 2014 at Iheya North, with 20 and 10 ovigerous individuals representing 37% and 6.8% of all the females collected at this vent field for each cruise, respectively. *A. longirostris* ovigerous females were found in every vent fields of the Okinawa trough except Futagoyama (see Table S1), in a period comprised between July and December (2010-2016) (6 to 19 females; Fig. 2 and Table 1). These ovigerous females represented between 15.2 and 36.4% of all *A. longirostris* females for Sakai and Tarama Knoll vent fields, respectively. Furthermore, a large proportion of *A. longirostris* ovigerous females was also found at the Off Hatsushima seep in the Sagami Bay both in February 2021 and 2022, but not in May 2022.

Fecundities and sizes at first reproduction

The realized fecundity of *O. loihi* and *A. longirostris* correlated positively with carapace length (Spearman's correlation: *O. loihi*: $r = 0.74$, $p < 0.0001$; *A. longirostris*: $r = 0.85$, $p < 0.0001$) but not for *S. leurokolos* (Spearman's correlation: *S. leurokolos*: $r = 0.25$, $p > 0.05$) (Fig. 4A.). A mean egg number of 185 eggs per broods was observed for *O. loihi*, 193 eggs for *S. leurokolos* and 1081 eggs for *A. longirostris*. Overall, size-specific relative fecundities ranged from 10.2 to 49.2 eggs mm^{-1} for *O. loihi*, from 3.1 to 51.8 eggs mm^{-1} for *S. leurokolos* and from 19.4 to 181 eggs mm^{-1} for *A. longirostris* (Fig 4B.). Large differences in size-specific fecundity were observed among the three species (Kruskal-Wallis $H = 79.38$, $p < 0.001$), with significantly greater size-specific fecundities in *A. longirostris* (Dunn's Multiple Comparison Test, $p < 0.001$) but similar size-specific fecundities between *O. loihi* and *S. leurokolos* (Dunn's Multiple Comparison Test, $p > 0.05$). These variations disappeared when individuals from a similar size range were compared (*A. longirostris* from Tarama Knoll: $CL = 6.44 \pm 2.38$ mm; *S. leurokolos* from Iheya North: $CL = 7.16 \pm 0.41$ mm; *O. loihi* from Suiyo: $CL = 6.02 \pm 0.64$ mm), with similar size-specific fecundities between *A. longirostris* from Tarama, *S. leurokolos* from Iheya North and *O. loihi* from Suiyo (Dunn's Multiple Comparison Test, $p > 0.05$). Similarly, large differences in size-specific fecundities of *A. longirostris* among the localities (Kruskal-Wallis $H = 23.508$, $p < 0.001$) were mostly related to variations in body size, with a smaller size-specific fecundity in *A. longirostris* from Tarama compared to the other sites and slightly higher size-specific fecundity in *A. longirostris* from Iheya North compared to most sites, except at Daisan Kume Knoll (Dunn's Multiple Comparison Tests, $p < 0.001$). Due to their limited sampling, statistical comparisons could not be performed for *A. dissimilis*, although they appeared to fall in the same range of relative fecundity as *O. loihi* and *A. longirostris* with 18.2 to 27.3 eggs mm^{-1} (131 eggs per brood in average) (Fig. 4A).

The observed size at the first reproduction (i.e., the smallest recorded ovigerous females) were also very similar among the four alvinocaridid species, ranging between 4.4 mm

CL for *A. dissimilis* and 5.3 mm CL for *A. longirostris* (Table 1). Notably, the smallest ovigerous females of *A. longirostris* showed a large size variation across sampling sites, ranging between 5.3 mm CL at Tarama Knoll and 10.3 mm CL at Izena Hole.

Egg stage proportions and egg volumes

Eggs within the same brood were found to exhibit synchronous development and were all at the same stage of development (early, mid, or late). However, there was no evidence of synchrony among broods of different females from the same sampling event (Fig. 4C). The majority of *O. loihi* broods collected at Suiyo in 2019 were at an early stage (52 broods; 53.6%) or a medium stage (40 broods; 41.2%), but there were also a limited number of late-stage broods (5 broods; 5.2%). Similarly, all *S. leurokolos* broods collected at Iheya North in 2013 and 2014 were at an early developmental stage (20 and 10 broods, respectively; Fig. 4C). Broods of *A. longirostris* from Okinawa vents were also mostly at early and mid-stages (17 broods and 18 broods respectively), with only three late-stage egg broods found at Tarama Knoll. In contrast, samples of *A. longirostris* from Off Hatsushima collected at almost a one-year interval showed clear differences in egg stage proportions, with only early and mid-stages egg broods found in February 2021 (6 broods in total) and only mid- and late-stage egg broods in February 2022 (8 broods in total; Fig. 4C).

Differences in egg volumes were observed among the three alvinocaridid species – *O. loihi*, *S. leurokolos*, and *A. longirostris* – for each stage of development (Kruskal-Wallis tests; early: $H = 30.95$, $p < 0.001$; mid: $H = 27.33$, $p < 0.001$; late: $H = 8.64$, $p < 0.01$), with larger egg volumes for *A. longirostris* compared to both *O. loihi* and *S. leurokolos* (Dunn's Multiple Comparison Test, $p < 0.001$) (Fig. 4D). In contrast, no significant variations in egg volumes were found among populations of *A. longirostris* from different sampling sites (Kruskal-Wallis tests; early stage: $H = 8.24$, $p > 0.05$; late stage: $H = 7.4$, $p > 0.05$), except for mid stage broods (Kruskal-Wallis $H = 13.93$, $p < 0.001$) with slightly larger egg volumes for *A. longirostris* from Off Hatsushima compared with those from Daisan Kume and Izena Hole (Dunn's Multiple Comparison Tests, $p < 0.05$).

Incubation experiments of *Opaepele loihi*

Eggs and larvae of *Opaepele loihi* exhibited negative buoyancy. The carapace of hatched *O. loihi* larvae was filled with orange yolk and lacked a prominent rostrum (Fig. 5A). The mean larval sizes were 0.76 ± 0.04 mm of carapace length (CL) and 2.40 ± 0.22 mm for total length ($n = 20$). Eyes were sessile with a red pigment spot in their center.

Incubations of *O. loihi* egg masses at 5°C were the closest to thermal conditions encountered by the brooding individuals in their habitat, where we measured a mean temperature of 5.2 ± 0.4 °C with peaks at 6.2°C in the mussel bed where specimens were collected (Fig. 5B). However, hatching rates were the highest under 10°C and 15°C for the three egg broods whereas none of the eggs hatched under 25°C and only a few at 20°C (Fig. 5C). Although most egg masses survived at 5°C until the end of the experiment, only a few egg masses of OL1 hatched at this temperature. Timing of hatching was congruent with embryonic stages

characterized at the beginning of the experiment, with earlier hatching for late-stage egg broods (OL1, early larval structures) compared with egg broods at an earlier developmental stage (OL5, early gastrulation; OL7, multicellular stage). Significant differences were seen between the temperature treatments, with shorter survival periods and shorter hatching rate in the warmer conditions (Fig. 5C).

Discussion

Four alvinocaridid species with contrasting population structure

Alvinocaridid shrimps from chemosynthetic ecosystems around Japan exhibited contrasting population structures among the three studied species. Whereas *O. loihi* population from Suiyo Seamount stood out by a clear dominance of juveniles, only a very limited number of these early life stages could be collected for *S. leurokolos* and *A. longirostris* (Fig. 2). Nonetheless, the three species all tended to exhibit sex ratios biased towards females, as generally seen in other alvinocaridid shrimps (Copley and Young 2006; Nye et al. 2013; Hernández-Ávila et al. 2022; Methou et al. 2022a).

Considering our limited sampling for each given site, we cannot exclude the possibility that these disequilibrated sex ratios and the scarcity of juvenile stages in *Shinkaicaris leurokolos* and *Alvinocaris longirostris* populations may be related to spatial segregation between life stages within different areas of the vent or seep sites. Our results indicate clear spatial variations between sexes in *S. leurokolos* populations from Iheya North among distinct sampling events. Differential distribution of males and females have been repeatedly reported for several crustaceans inhabiting deep-sea vents and seeps (Copley and Young 2006; Marsh et al. 2015; Hernández-Ávila et al. 2022; Methou et al. 2022a), agreeing with the biases seen in our results. These spatial segregations are generally associated with variable environmental parameters, with males being preferentially distributed in the hottest part of the vent fields in *Kiwa tyleri* yeti crabs (Marsh et al. 2015), closer to sulfidic extremes in *Alvinocaris stactophila* shrimps (Copley and Young 2006), or away from the vent fluid activity in *Rimicaris exoculata* (Hernández-Ávila et al. 2022; Methou et al. 2022a). Similar observations could not be established among *S. leurokolos* samples from Iheya North and further environmental characterization of their habitat would be required to understand if spatial distributions of the two sexes in this species are also associated with flux in environmental parameters. Segregation between juveniles and adults is also known from alvinocaridid species in the genus *Rimicaris* from the Mid-Atlantic Ridge where juveniles aggregate at specific nurseries habitats at the periphery of their adult populations (Hernández-Ávila et al. 2022; Methou et al. 2022a). This was true for both *Rimicaris exoculata* whose adults inhabit live near hot, vigorous fluid emissions and *R. chacei* inhabiting cooler areas around mussel beds. Nevertheless, these demographic patterns are in contrast with those observed in *O. loihi* population from Suiyo, for which both sexes and juvenile stages were all found mixed within the same sampling location.

Distinct mortality rates between adult and juveniles and/or between sexes is another potential factor that may lead to the observed differences in demographic structures among alvinocaridid species. For instance, a strong collapse of *R. chacei* population following

recruitment attributed to high juvenile mortality due to size-specific predation and/or competitive processes with *R. exoculata*, a co-occurring alvinocaridid species (Methou et al. 2022a), has been suggested to cause a population structure similar to the *O. loihi* population structure seen herein. Variations in larval supply, either in term of timing or number of larval settlers, may also exist among the four species investigate here, as suggested by the observed differences in their reproductive traits.

An early maturity but similar reproductive traits than other alvinocaridids

The four alvinocaridid species from the northwestern Pacific were gonochoric and exhibited sexual dimorphism, consistent with all other alvinocaridid species studied to date. Overall, they were characterized by small sizes at maturity (i.e. sizes of their smallest ovigerous females) being similar to their minimum sexable sizes or even sizes of their smallest recruits (minimum juvenile sizes) (Table 1). This is in striking contrast with most previously examined alvinocaridids from the Atlantic and Indian oceans, which exhibit greater difference between the observed minimum size of ovigerous females (*R. exoculata*: 12 mm, *R. chacei*: 11.8 mm, *R. kairei*: 18.1 mm) and the sizes of their smaller adults (*R. exoculata*: 10 mm, *R. chacei*: 5.98 mm, *R. kairei*: 10 mm) (Nye et al. 2013; Methou et al. 2022b, a). Size at first maturity is often considered a key life-history trait generally proportional to the maximum body size and reflects the reproductive investment of a species (Anger and Moreria 1998). These Pacific alvinocaridids may therefore have higher reproductive investment than species from other regions, although this should be confirmed with metabolic budget modeling (Gaudron et al. 2021). This trend was most clearly observed for *Alvinocaris longirostris* with significant disparities between sizes at onset of maturity and minimum sexable sizes among its different populations (Table 1). We note that similar sizes variations were also found in *Rimicaris hybisae* across different sites (Nye et al. 2013), implying conspecific populations of alvinocaridids could mature at different sizes and differ in their reproductive investment.

Despite wide variations in average body sizes of their ovigerous stages, *A. longirostris*, *O. loihi* and *S. leurokolos* exhibited similar size-specific fecundities, ranging from 10.2 to 49.2 eggs mm⁻¹ for *O. loihi*, from 3.1 to 51.8 eggs mm⁻¹ for *S. leurokolos* and from 19.4 to 181 eggs mm⁻¹ for *A. longirostris* (Fig. 4A). This trend was even clearer when ovigerous females of *O. loihi* or *S. leurokolos* were compared with those of *A. longirostris* from Tarama Knoll which were of similar sizes. No variations could be seen either in the fecundities of *A. longirostris* from the Off Hatsushima seeps and those from hydrothermal vents at similar size ranges (Fig. 4B). Previous studies of alvinocaridid shrimps have emphasized the possible influence of feeding strategies on fecundities in addition to body size (Methou et al. 2022b), with overall lower size-specific fecundities in fully chemosymbiotic species compared with species that have a mixotrophic diet (Nye et al. 2013; Methou et al. 2022b). Although we currently have limited knowledge on the feeding strategies of alvinocaridids from chemosynthetic ecosystems around Japan, we observed *O. loihi* individuals grazing bacterial mats covering *Bathymodiolus septemdierum* mussels (supplementary video material S1), suggesting either full bacterivory or a mixed diet for this species. These observations are also consistent with stable isotopic ratios and lipid compositions of *O. loihi* populations from distinct vent sites on the Mariana Arc (Stevens et al.

2008). Additionally, *A. longirostris* was characterized as grazers/scavengers in a Manus Basin vent study according to their isotopic ratios (Van Audenhaege et al. 2019). As *O. loihi* and *A. longirostris* exhibited similar size-specific fecundity to other mixotrophic alvinocaridid like *R. chacei* (Methou et al. 2022b), our results give further support to the hypothesis that fecundities in alvinocaridid shrimps could be partially driven by their feeding strategies and thus the availability of food supply for each species. Additional information on the diet of *S. leurokolos* across size ranges and life stages is required to understand if they fit within this framework as well.

Our results also indicated significant differences in egg volumes between the two species, with slightly larger egg volumes for *A. longirostris* compared to *O. loihi* of similar embryonic stages. Although these variations remain limited, these observations indicate that the egg size of *A. longirostris* is large among alvinocaridid shrimps while *O. loihi* egg sizes are among the smaller ones in the family (Ramirez-Llodra and Segonzac 2006; Copley and Young 2006; Nye et al. 2013; Methou et al. 2022b). However, these variations in egg sizes among species do not appear to be reflected in the size of their first zoea larval stages, with the *O. loihi* hatched larva exhibiting carapace sizes or total sizes similar to those seen in *R. exoculata* or *M. fortunata* hatched larva (Hernández-Ávila et al. 2015) despite larger mean egg sizes than *O. loihi* for these two species (Ramirez-Llodra et al. 2000; Methou et al. 2022b). Therefore, these similar sizes of hatched larvae in all alvinocaridids examined so far, with also similar yolk reserves, indicate that they probably all undergo an early lecithotrophic phase followed by an extended larval development (Hernández-Ávila et al. 2015). This suggest that the egg size may have limited feasibility in estimating the dispersal capability in this group.

Egg incubation experiment confirmed the strong influence of temperature on brooding duration and hatching rate of *O. loihi* egg masses, as previously observed in *S. leurokolos* and *A. longirostris* (Watanabe et al. 2016), other vent species (Pradillon et al. 2001), and decapods from other ecosystems (Tong et al. 2000; Brillon et al. 2005; García-Guerrero 2010). This influence of temperature on these parameters is species-specific in alvinocaridids, with successful hatchings between 5°C and 15°C for *A. longirostris* and above 10°C for *S. leurokolos* (Watanabe et al. 2016). Our experiments on *O. loihi* egg broods revealed an intermediate response, with successful hatchings at 10°C and 15°C but nearly no hatching at 5°C or at conditions above 15°C. Since these species occupy different thermal niches in their habitat (Yahagi et al. 2015), it can be assumed that they display distinct brooding durations in their natural environment. Thus, the distribution of *S. leurokolos* ovigerous stages in warmer areas close to venting orifices could result in a faster egg development and shorter brooding durations than *O. loihi* and *A. longirostris* inhabiting more peripheral and colder areas within the vent field. Nonetheless, the near absence of hatching at 5°C for *O. loihi* in the incubation experiments was unexpected given that these thermal conditions were the closest to those measured during sampling within their mussel bed habitat (Fig. 5B). It is possible that this one-shot temperature measurement do not represent the full thermal range experienced by *O. loihi* ovigerous females, which could move occasionally toward warmer habitats during their brooding phase. Additional biases could also have arisen from the absence of pressure in our experimental design to reproduce the environmental

conditions experienced by *O. loihi* at hatching (138 atm for populations from Suiyo, 1380m depth). Previous larval rearing experiments of *M. fortunata* inhabiting similar depth revealed a combined effect of temperature and pressure on larva survival, with different survival success according to depth for a set temperature (Tyler and Dixon 2000). Since all hatched larvae of *O. loihi* were unable to swim in our laboratory experiments, it is possible that they were physiologically impacted, though they were able to actively move their thoracic appendages. Additional *in situ* measurements around *O. loihi* ovigerous females and further egg incubation experiments using pressure chambers will be needed to better explore this apparent discrepancy between our results.

Perspectives on reproductive timing of alvinocaridid shrimps: When and how long?

By precisely characterizing the developmental stages of the egg masses at the start of our incubation experiment, we were able to obtain a first estimation of the brooding duration for *Opaepele loihi*. We defined these durations by determining the timing when most larvae hatched – the point when hatching rates reached a plateau – at 10°C. Given that the experiment at 5°C was unsuccessful (6 out of 50 in one brood and none in the other hatched), the 10°C condition was the closest successful experiment condition to the natural habitat temperature (around 5-6°C) (Fig. 6A). This gave a total duration of approximately 79 days from the multicellular stage before gastrulation until larval hatching. This therefore implies a duration of about 63 days from the nauplius stage (mid stage) and 53 days from the appearance of the first larval structures (late stages). Although incomplete with the timing preceding the blastula missing, this brooding duration is relatively short in comparison with other decapods incubated in similar thermal ranges (Tong et al. 2000; Brillon et al. 2005; García-Guerrero 2010). Our data also suggests that even in the case of continuous reproduction throughout the year, each female *O. loihi* shrimp cannot have more than four broods per year under similar thermal conditions.

Although our dataset did not allow us to precisely determine brooding cycles, we could still investigate hypotheses on the reproductive periodicity of alvinocaridids from Okinawa Trough vents and a Sagami Bay seep by summarizing the occurrence of ovigerous females in our samplings (Fig. 6B and 6C). The repeated presence of ovigerous stages in most of our samples suggests an aperiodic brooding cycle throughout the year in *A. longirostris* (Fig. 6B). In contrast, collecting events of *S. leurokolos* ovigerous females were mostly limited to November and January with a limited number of these reproductive stages outside this period of the year (Fig. 6C). Although oocyte size-frequency distribution among individual *S. leurokolos* within samples did not appear to follow a periodic reproductive pattern, these results on the occurrence of their ovigerous stages suggest a possible periodicity of their brooding phase. Similar inconsistencies were already observed in *R. exoculata*, which exhibits lacks synchronicity for their gametogenesis phase (Ramirez-Llodra et al. 2000; Copley et al. 2007) but displays a periodicity for their brooding phase between January and April (Hernández-Ávila et al. 2022; Methou et al. 2022a). Additional sampling of alvinocaridid shrimps across different seasons of the year is required to confirm these reproductive patterns suggested by the results of the present study.

Updated geographical distribution with range extensions

We report two new localities for *A. dissimilis*, previously known only from the Minami Ensei vent field (Komai and Segonzac 2005), at the Kuroshima Knoll methane seep and the Higashi Aogashima vent field, consistent with a distribution restricted to relatively shallow sites (641 – 750 m depth) although these were separated by large distances (between 585 and 1280 kms with the closest site) (Fig. 1). The vent crab *Gandalfus yunohana* was once thought to be only found on the IBM Arc but one individual with no genetic differentiation was later found in an Okinawa Trough vent (Watanabe et al. 2020). Its rarity in Okinawa was implied to be a result of low larval supply and perhaps a lack of reproductive population. The COI sequence of the *A. dissimilis* from Higashi Aogashima field and the Kuroshima Knoll was identical with many individuals from the Minami Ensei vent field (Yahagi et al. 2015), suggesting high genetic connectivity. Since we collected 11 individuals from Higashi Aogashima, this suggests reproductive populations are present at both Okinawa and Izu-Ogasawara for this species, unlike *G. yunohana*. The two species may disperse at different depth layers or have very different dispersal capabilities.

We also extended the reported distribution of *O. loihi* to Suiyo Seamount on the IBM Arcs, 630 km north of its previous northernmost record at Nikko Seamount (Komai and Tsuchida 2015) (Fig. 1). Combining with previous records of alvinocaridid shrimps in the northwestern Pacific (Nakajima et al. 2014; Watanabe et al. 2019; Brunner et al. 2022), this suggests that the genus *Alvinocaris* is widely distributed across both vents and seeps in Okinawa Trough, Sagami Bay, and IBM Arcs, while *Shinkaicaris* is limited to Okinawa Trough vents and *Opaepele* is restricted to the IBM Arc vents. These new records also reveal that *A. dissimilis* are not endemic to vents but can inhabit other chemosynthetic ecosystems such as methane seeps, as seen in a few other *Alvinocaris* species such as *A. longirostris* (Yahagi et al. 2015) or the *A. muricola/A. markensis* species complex (Teixeira et al. 2013; Pereira et al. 2020).

Acknowledgments

We thank the captains and crews of numerous research cruises conducted on-board R/V *Kairei* (KR15-16, KR15-17, KR16-16), R/V *Natsushima* (NT05-05, NT10-17, NT13-22, NT15-13), R/V *Kaiyo* (KY14-01), R/V *Yokosuka* (YK17-17, YK19-10, YK22-05), and R/V *Shinsei-Maru* (KS-21-20, KS-22-2). We also thank the pilots and the operation team of the HOV *Shinkai 6500* and of the ROVs *Kaiko*, *Hyper-Dolphin*, and *KM-ROV* during these research cruises. We gratefully acknowledge the chief scientists of the relevant expeditions: Shinsuke Kawagucci (JAMSTEC; NT10-17, KR15-16), Hironori Komatsu (National Museum of Nature and Science, Tsukuba; KS-22-2), Hiroko Makita (JAMSTEC and Tokyo University of Marine Science and Technology; YK17-17), Junichi Miyazaki (JAMSTEC; KR16-16), Tatsuo Nozaki (JAMSTEC; KS-21-20), Ken Takai (JAMSTEC; NT15-13, KY14-01, YK19-10, YK22-05), Hiroyuki Yamamoto (JAMSTEC; NT13-22, KR15-17).

Authors' contributions

P.M. collected specimens from the KS-21-20 expedition, carried out the identification of shrimps, including molecular barcoding, and measurement of specimens from all sampling cruises except NT13-22 and KY14-01, lead the data analysis, participated in the conception and design of the study and drafted the original manuscript; V.N. conducted identification, measurements and data analysis of specimens collected during NT13-22 and KY14-01 cruises, participated in the design of the study and critically revised the manuscript; J.C. participated in the design of the study and critically revised the manuscript. H.K.W. carried out the collection of specimens from YK19-10, designed and conducted *in vitro* egg incubation experiment and its analysis, and critically revised the manuscript. Y.N. conducted the *in vitro* egg incubation experiment, and critically revised the manuscript. C.C. collected and sorted materials from most of the relevant expeditions, assisted in drafting the original manuscript, and coordinated the study. All authors gave final approval for submission and publication of the manuscript in its current form.

Data availability

All genetic sequences have been deposited in GenBank under accession numbers OP482454 to OP482487. Dataset on population and reproductive traits are available on the figshare repository: 10.6084/m9.figshare.21345183

Funding

PM was supported by a JAMSTEC Young Research Fellow fellowship. CC and HKW were supported by a Grant-in-Aid for Scientific Research (KAKENHI) from the Japan Society for the Promotion of Science (JSPS), grant code 18K06401.

Ethics

Faunal collections were conducted in Japanese exclusive economic zone by Japanese government research vessels. Research animals were invertebrate caridean shrimps and no live experiments with animals were conducted in this study.

Conflict of interest

We have no conflict of interest.

Figure Caption

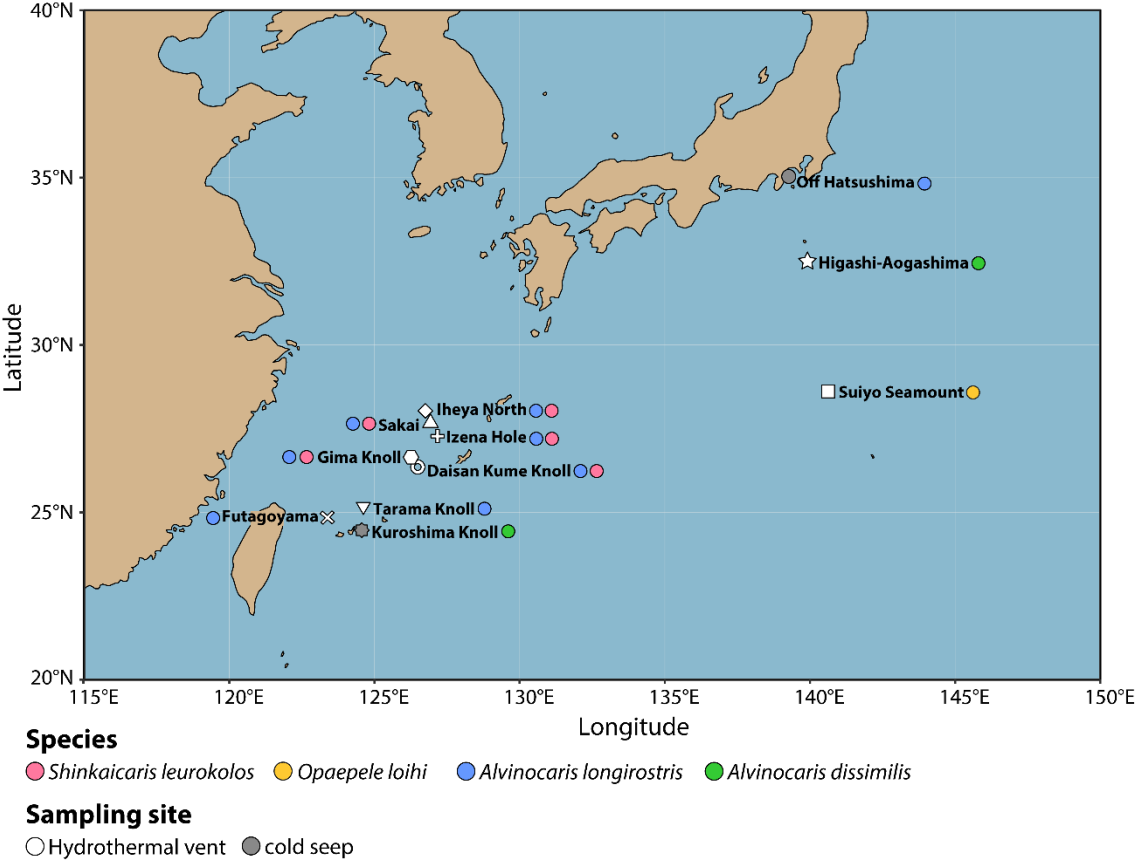
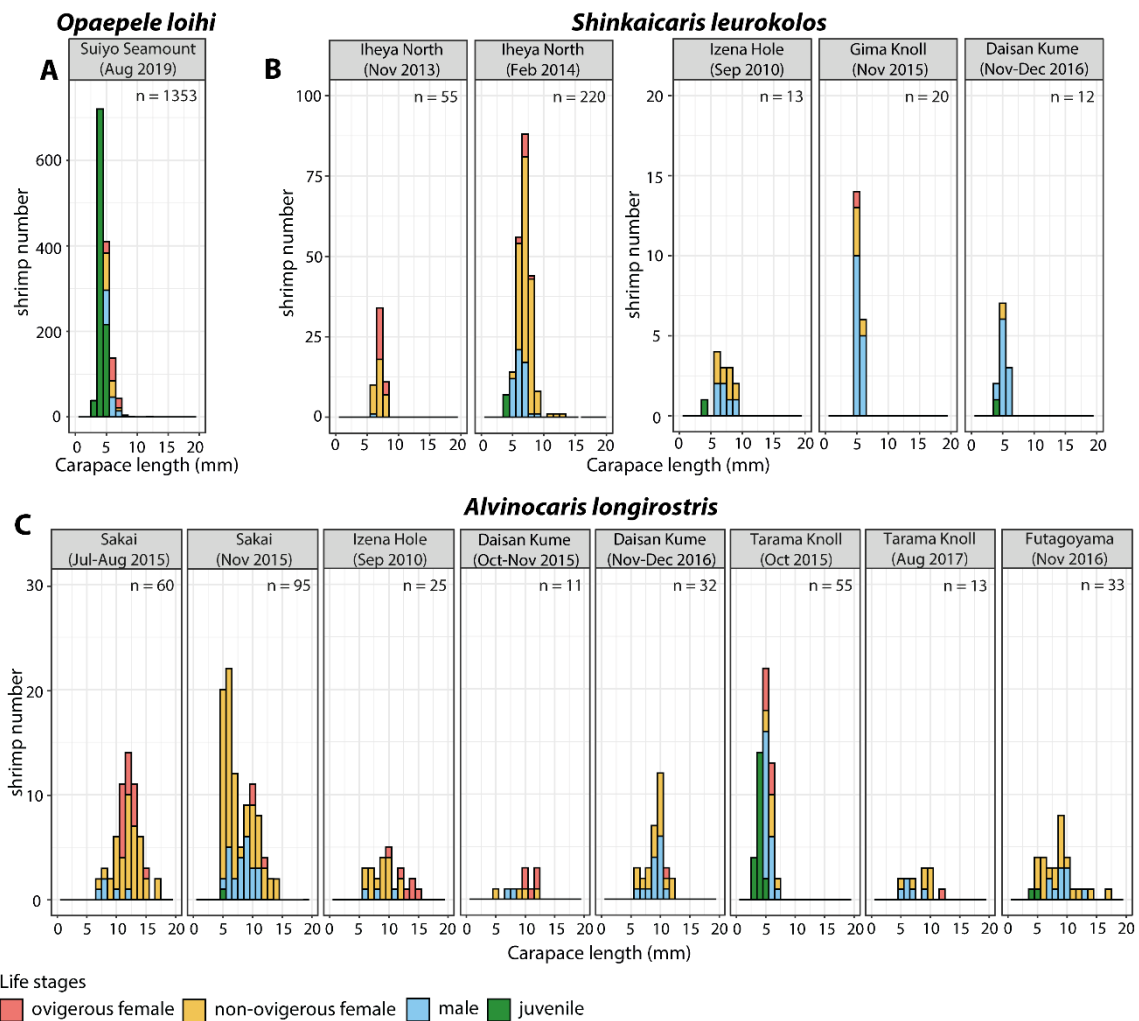


Figure 1. Map of sampling localities for the five alvinocaridid species analysed in this study.



Life stages
ovigerous female non-ovigerous female male juvenile

Figure 2. Size-frequency distribution of the four alvinocaridid shrimps investigated, denoting sexes and reproductive stages: **A.** *Opaepele loihi* **B.** *Shinkaicaris leurokolos* **C.** *Alvinocaris longirostris*. **D.** *Alvinocaris dissimilis*.

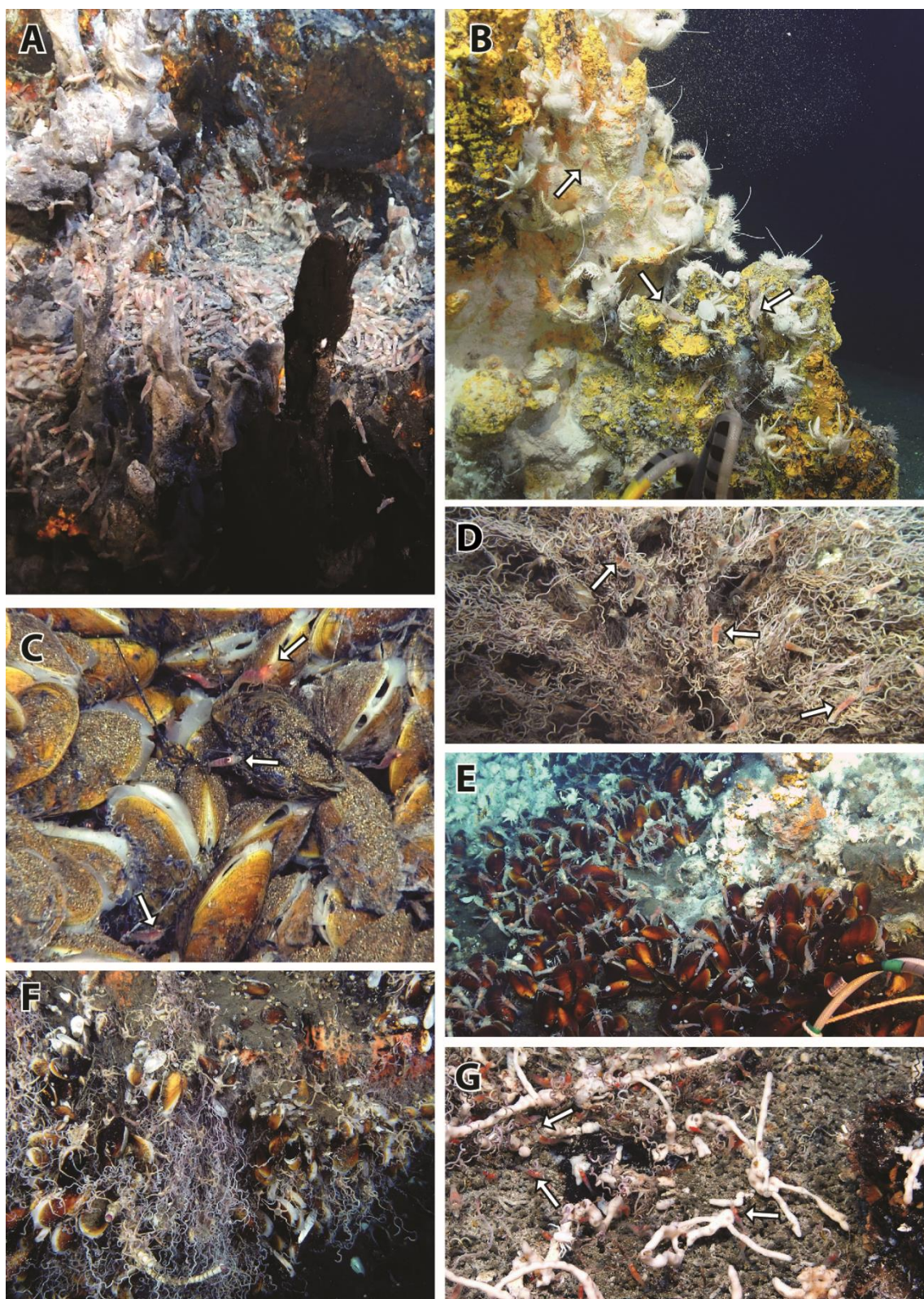


Figure 3. Overview of the different assemblages from hydrothermal vent fields and seeps off Japan where alvinocaridid shrimps could be collected. **A.** Aggregation of *Shinkaicaris leurokolos* near vent fluid exits at the Yokosuka site, Okinawa Trough. **B.** *Alvinocaris longirostris* on chimney

rocks in close vicinity with *Shinkaia crosnieri* squat lobsters at the Daisan Kume Knoll, Okinawa Trough. **C.** *Opaepele loihi* within a *Bathymodiolus septemdiarum* mussel bed at Suiyo Seamount, Izu-Ogasawara Arc. **D.** *Alvinocaris* spp. on a tubeworm bush at Sakai field, Okinawa Trough. **E.** *Alvinocaris longirostris* on a mussel bed at Futagoyama field, Okinawa Trough. **F.** *Alvinocaris longirostris* hidden in a tubeworm bush at the Off Hatsushima seep, Sagami Bay. **G.** *Alvinocaris longirostris* within a branching sponge colony at Tarama Knoll, Okinawa Trough.

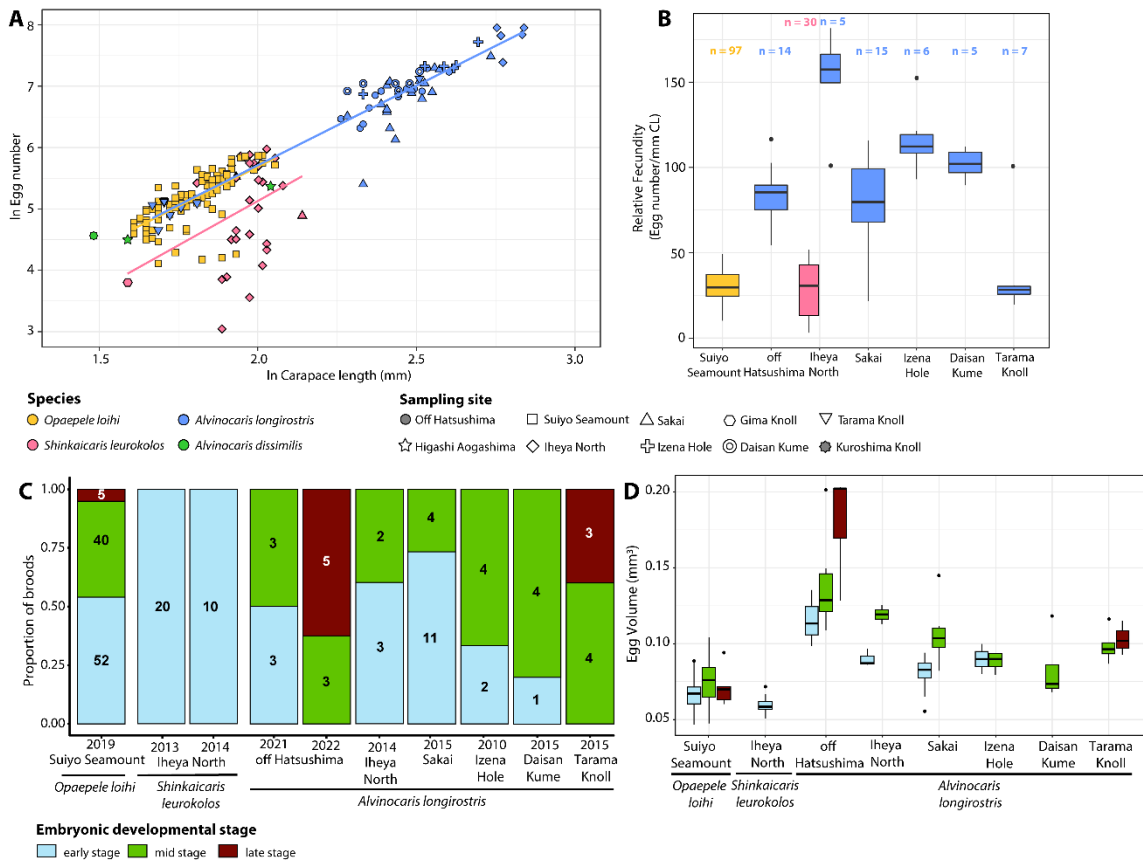


Figure 4. Comparison of reproductive features between alvinocaridid species from hydrothermal vents fields off Japan. **n:** number of individuals for each condition. **A.** Variation of \log_e -transformed minimum realized fecundity with \log_e -transformed carapace length. **B.** Fecundity corrected for body size (carapace length). **C.** Proportions of each egg developmental stages. Numbers within the plots indicates the number of broods per developmental stages. **D.** Egg volumes at different stages.

629

630 **References**

- 631 Anger K, Moreria GS (1998) Morphometric and reproductive traits of tropical caridean shrimps.
632 J Crustac Biol 18:823–838. doi: 10.2307/1549156
- 633 Beedessee G, Watanabe H, Ogura T, Nemoto S, Yahagi T, Nakagawa S, Nakamura K, Takai K,
634 Koonjul M, Marie DEP (2013) High Connectivity of Animal Populations in Deep-Sea
635 Hydrothermal Vent Fields in the Central Indian Ridge Relevant to Its Geological Setting.
636 PLoS One 8:e81570. doi: 10.1371/journal.pone.0081570
- 637 Brillon S, Lambert Y, Dodson J (2005) Egg survival, embryonic development, and larval
638 characteristics of northern shrimp (*Pandalus borealis*) females subject to different
639 temperature and feeding conditions. Mar Biol 147:895–911. doi: 10.1007/s00227-005-
640 1633-6
- 641 Brunner O, Chen C, Giguère T, Kawagucci S, Tunnicliffe V, Kayama H, Satoshi W (2022) Species
642 assemblage networks identify regional connectivity pathways among hydrothermal vents
643 in the Northwest Pacific. Ecol Evol 1–15. doi: 10.1002/ece3.9612
- 644 Copley JTP, Young CM (2006) Seasonality and zonation in the reproductive biology and
645 population structure of the shrimp *Alvinocaris stactophila* (Caridea: Alvinocarididae) at a
646 Louisiana Slope cold seep. Mar Ecol Prog Ser 315:199–209. doi: 10.3354/meps315199
- 647 Copley JTP, Jorgensen PBK, Sohn RA (2007) Assessment of decadal-scale ecological change at a
648 deep Mid-Atlantic hydrothermal vent and reproductive time-series in the shrimp
649 *Rimicaris exoculata*. J Mar Biol Assoc 87:859–867. doi: 10.1017/S0025315407056512
- 650 Cowen RK, Sponaugle S (2009) Larval Dispersal and Marine Population Connectivity. Ann Rev
651 Mar Sci 1:443–466. doi: 10.1146/annurev.marine.010908.163757
- 652 Danovaro R, Fanelli E, Aguzzi J, Billett D, Carugati L, Corinaldesi C, Dell’Anno A, Gjerde K,
653 Jamieson AJ, Kark S, McClain C, Levin L, Levin N, Ramirez-Llodra E, Ruhl H, Smith CR,
654 Snelgrove PVR, Thomsen L, Van Dover CL, Yasuhara M (2020) Ecological variables for
655 developing a global deep-ocean monitoring and conservation strategy. Nat Ecol Evol
656 4:181–192. doi: 10.1038/s41559-019-1091-z
- 657 García-Guerrero MU (2010) Effect of temperature on consumption rate of main yolk
658 components during embryo development of the prawn *Macrobrachium americanum*
659 (Crustacea: Decapoda: Palaemonidae). J World Aquac Soc 41:84–92. doi: 10.1111/j.1749-
660 7345.2009.00336.x
- 661 Gaudron SM, Lefebvre S, Marques GM (2021) Inferring functional traits in a deep - sea wood -
662 boring bivalve using dynamic energy budget theory. Sci Rep 1–13. doi: 10.1038/s41598-
663 021-02243-w
- 664 Gollner S, Colaço A, Gebruk A, Halpin PN, Higgs N, Menini E, Mestre NC, Qian PY, Sarrazin J,
665 Szafranski K, Van Dover CL (2021) Application of scientific criteria for identifying
666 hydrothermal ecosystems in need of protection. Mar Policy 132:104641. doi:
667 10.1016/j.marpol.2021.104641
- 668 Hernández-Ávila I, Cambon-Bonavita MA, Pradillon F (2015) Morphology of first zoeal stage of

669 four genera of alvinocaridid shrimps from hydrothermal vents and cold seeps:
 670 Implications for ecology, larval biology and phylogeny. PLoS One 10:1–27. doi:
 671 10.1371/journal.pone.0144657

672 Hernández-Ávila I, Cambon-Bonavita M-A, Sarrazin J, Pradillon F (2022) Population structure
 673 and reproduction of the alvinocaridid shrimp *Rimicaris exoculata* on the Mid-Atlantic
 674 Ridge: variations between habitats and vent fields. Deep Sea Res Part I Oceanogr Res Pap
 675 186:3–5. doi: 10.1016/j.dsr.2022.103827

676 Husson B, Sarrazin PM, Zeppilli D, Sarrazin J (2017) Picturing thermal niches and biomass of
 677 hydrothermal vent species. Deep Res Part II Top Stud Oceanogr 137:6–25. doi:
 678 10.1016/j.dsr2.2016.05.028

679 Jollivet D, Empis A, Baker MC, Hourdez S, Comtet T, Desbruyères D, Tyler PA (2000)
 680 Reproductive biology, sexual dimorphism, and population structure of the deep sea
 681 hydrothermal vent scale-worm, *Branchipolynoe seepensis* (Polychaeta : Polynoidae). J
 682 Mar Biol Assoc United Kingdom 80:55–68. doi: 10.1017/S0025315499001563

683 Ke Z, Li R, Chen Y, Chen D, Chen Z, Lian X, Tan Y (2022) A preliminary study of macrofaunal
 684 communities and their carbon and nitrogen stable isotopes in the Haima cold seeps,
 685 South China Sea. Deep Res Part I Oceanogr Res Pap 184:103774. doi:
 686 10.1016/j.dsr.2022.103774

687 Kelly NE, Metaxas A (2007) Population structure of two deep-sea hydrothermal vent
 688 gastropods from the Juan de Fuca Ridge, NE Pacific. Mar Biol 153:457–471. doi:
 689 10.1007/s00227-007-0828-4

690 Komai T, Segonzac M (2005) A revision of the genus *Alvinocaris* Williams and Chace (Crustacea:
 691 Decapoda: Caridea: Alvinocarididae), with descriptions of a new genus and a new species
 692 of *Alvinocaris*. J Nat Hist 39:1111–1175. doi: 10.1080/00222930400002499

693 Komai T, Tsuchida S (2015) New records of Alvinocarididae (Crustacea: Decapoda: Caridea)
 694 from the southwestern Pacific hydrothermal vents, with descriptions of one new genus
 695 and three new species. J Nat Hist 1–36. doi: 10.1080/00222933.2015.1006702

696 Li X (2015) Report on two deep-water caridean shrimp species (Crustacea: Decapoda: Caridea:
 697 Alvinocarididae, Acanthephyridae) from the northeastern South China Sea. Zootaxa
 698 3911:130–138. doi: 10.11646/zootaxa.3911.1.8

699 Lunina AA, Vereshchaka AL (2014) Distribution of hydrothermal alvinocaridid shrimps: Effect of
 700 geomorphology and specialization to extreme biotopes. PLoS One. doi:
 701 10.1371/journal.pone.0092802

702 Macdonald P, Du J (2012) Mixdist: finite mixture distribution models.

703 Marsh L, Copley JT, Tyler PA, Thatje S (2015) In hot and cold water: Differential life-history
 704 traits are key to success in contrasting thermal deep-sea environments. J Anim Ecol
 705 84:898–913. doi: 10.1111/1365-2656.12337

706 Methou P (2019) Lifecycles of two hydrothermal vent shrimps from the Mid-Atlantic Ridge:
 707 *Rimicaris exoculata* and *Rimicaris chacei*.

708 Methou P, Michel LN, Segonzac M, Cambon-Bonavita M-A, Pradillon F (2020) Integrative
 709 taxonomy revisits the ontogeny and trophic niches of *Rimicaris* vent shrimps. R Soc Open

710 Sci 7:200837. doi: 10.1098/rsos.200837

711 Methou P, Hernández-Ávila I, Cathalot C, Cambon-Bonavita M-A, Pradillon F (2022a)

712 Population structure and environmental niches of Rimicaris shrimps from the Mid-

713 Atlantic Ridge. Mar Ecol Prog Ser 684:1–20. doi: 10.3354/meps13986

714 Methou P, Chen C, Kayama H, Cambon M-A, Pradillon F (2022b) Reproduction in deep-sea vent

715 shrimps is influenced by diet, with rhythms apparently unlinked to surface production.

716 Ecol Evol 1–12. doi: 10.1002/ece3.9076

717 Miller KA, Thompson KF, Johnston P, Santillo D (2018) An overview of seabed mining including

718 the current state of development, environmental impacts, and knowledge gaps. Front

719 Mar Sci. doi: 10.3389/fmars.2017.00418

720 Mullineaux LS, Metaxas A, Beaulieu SE, Bright M, Gollner S, Grupe BM, Herrera S, Kellner JB,

721 Levin LA, Mitarai S, Neubert MG, Thurnherr AM, Tunnicliffe V, Watanabe HK, Won YJ

722 (2018) Exploring the ecology of deep-sea hydrothermal vents in a metacommunity

723 framework. Front Mar Sci. doi: 10.3389/fmars.2018.00049

724 Nakajima R, Yamakita T, Watanabe H, Fujikura K, Tanaka K, Yamamoto H, Shirayama Y (2014)

725 Species richness and community structure of benthic macrofauna and megafauna in the

726 deep-sea chemosynthetic ecosystems around the Japanese archipelago: An attempt to

727 identify priority areas for conservation. Divers Distrib 20:1160–1172. doi:

728 10.1111/ddi.12204

729 Nye V, Copley JTP, Tyler PA (2013) Spatial Variation in the Population Structure and

730 Reproductive Biology of Rimicaris hybisae (Caridea: Alvinocarididae) at Hydrothermal

731 Vents on the Mid-Cayman Spreading Centre. PLoS One. doi:

732 10.1371/journal.pone.0060319

733 Pereira OS, Shimabukuro M, Bernardino AF, Gomes Sumida PY (2020) Molecular affinity of

734 Southwest Atlantic Alvinocaris muricola with Atlantic Equatorial Belt populations. Deep

735 Res Part I Oceanogr Res Pap 103343. doi: 10.1016/j.dsr.2020.103343

736 Pond DW, Dixon DR, Bell M V., Fallick AE, Sargent JR, David W, Sargentl JR (1997) Occurrence

737 of 16:2(n-4) and 18:2(n-4) fatty acids in the lipids of the hydrothermal vent shrimps

738 Rimicaris exoculata and Alvinocaris markensis: nutritional nutritional and trophic

739 implications. Mar Ecol Prog Ser 156:167–174. doi: 10.3354/meps156167

740 Pradillon F, Shillito B, Young CM, Gaill F (2001) Developmental arrest in vent worm embryos.

741 Nature 413:698–699. doi: 10.1038/35099674

742 R Core Team . (2020) R: A language and environment for statistical computing. [https://www.r-](https://www.r-project.org)

743 [project.org](https://www.r-project.org).

744 Ramirez-Llodra E, Segonzac M (2006) Reproductive biology of Alvinocaris muricola (Decapoda:

745 Caridea: Alvinocarididae) from cold seeps in the Congo Basin. J Mar Biol Assoc United

746 Kingdom 86:1347. doi: 10.1017/S0025315406014378

747 Ramirez-Llodra E, Tyler PA, Copley JTP (2000) Reproductive biology of three caridean shrimp,

748 Rimicaris exoculata, Chorocaris chacei and Mirocaris fortunata. J Mar Biol Assoc United

749 Kingdom 80:473–484. doi: 10.1017/S0025315400002174

750 Stevens CJ, Limén H, Pond DW, Gélinas Y, Juniper SK (2008) Ontogenetic shifts in the trophic

ecology of two alvinocaridid shrimp species at hydrothermal vents on the Mariana Arc, western Pacific Ocean. *Mar Ecol Prog Ser* 356:225–237. doi: 10.3354/meps07270

Teixeira S, Serrão EA, Arnaud-Haond S (2012) Panmixia in a fragmented and unstable environment: The hydrothermal shrimp *Rimicaris exoculata* disperses extensively along the Mid-Atlantic ridge. *PLoS One* 7:1–10. doi: 10.1371/journal.pone.0038521

Teixeira S, Olu K, Decker C, Cunha RL, Fuchs S, Hourdez S, Serrão EA, Arnaud-Haond S (2013) High connectivity across the fragmented chemosynthetic ecosystems of the deep Atlantic Equatorial Belt: Efficient dispersal mechanisms or questionable endemism? *Mol Ecol* 22:4663–4680. doi: 10.1111/mec.12419

Thaler AD, Plouviez S, Saleu W, Alei F, Jacobson A, Boyle EA, Schultz TF, Carlsson J, Van Dover CL (2014) Comparative population structure of two deep-sea hydrothermal-vent-associated decapods (*Chorocaris* sp. 2 and *Munidopsis lauensis*) from southwestern Pacific back-arc basins. *PLoS One* 9:1–13. doi: 10.1371/journal.pone.0101345

Tong LJ, Moss GA, Pickering TD, Paewai MP (2000) Temperature effects on embryo and early larval development of the spiny lobster *Jasus edwardsii*, and description of a method to predict larval hatch times. *Mar Freshw Res* 51:243–248. doi: 10.1071/MF99049

Tyler PA, Dixon DR (2000) Temperature/pressure tolerance of the first larval stage of *Mirocaris fortunata* from Lucky Strike hydrothermal vent field. *J Mar Biol Assoc United Kingdom* 80:739–740. doi: 10.1017/S0025315400002605

Van Audenhaege L, Fariñas-Bermejo A, Schultz T, Lee Van Dover C (2019) An environmental baseline for food webs at deep-sea hydrothermal vents in Manus Basin (Papua New Guinea). *Deep Res Part I Oceanogr Res Pap* 148:88–99. doi: 10.1016/j.dsr.2019.04.018

Van Dover CL (2019) Inactive Sulfide Ecosystems in the Deep Sea : A Review. *Front Mar Sci* 6:1–40. doi: 10.3389/fmars.2019.00461

Van Dover CL, Trask JL (2000) Diversity at deep-sea hydrothermal vent and intertidal mussel beds. *Mar Ecol Prog Ser* 195:169–178. doi: 10.3354/meps195169

Van Dover CL, Arnaud-Haond S, Gianni M, Helmreich S, Huber JA, Jaeckel AL, Metaxas A, Pendleton LH, Petersen S, Ramirez-Llodra E, Steinberg PE, Tunnicliffe V, Yamamoto H (2018) Scientific Rationale and International Obligations for Protection of Active Hydrothermal Vent Ecosystems From Deep-Sea Mining. *Mar Policy* 90:20–28. doi: 10.1016/j.marpol.2018.01.020

Vrijenhoek RC (2010) Genetic diversity and connectivity of deep-sea hydrothermal vent metapopulations. *Mol Ecol* 19:4391–4411. doi: 10.1111/j.1365-294X.2010.04789.x

Watanabe H, Yahagi T, Nagai Y, Seo M, Kojima S, Ishibashi J, Yamamoto H, Fujikura K, Mitarai S, Toyofuku T (2016) Different thermal preferences for brooding and larval dispersal of two neighboring shrimps in deep-sea hydrothermal vent fields. *Mar Ecol* 37:1282–1289. doi: 10.1111/maec.12318

Watanabe HK, Shigeno S, Fujikura K, Matsui T, Kato S, Yamamoto H (2019) Faunal composition of deep-sea hydrothermal vent fields on the Izu–Bonin–Mariana Arc, northwestern Pacific. *Deep Res Part I Oceanogr Res Pap* 149:103050. doi: 10.1016/j.dsr.2019.05.010

Watanabe HK, Chen C, Kojima S, Kato S, Yamamoto H (2020) Population connectivity of the

792 crab *Gandalfus yunohana* from deep-sea hydrothermal vents in the northwestern Pacific.
793 *J Crustac Biol* 1–7. doi: 10.1093/jcbiol/ruaa045

794 Yahagi T, Watanabe H, Ishibashi JI, Kojima S (2015) Genetic population structure of four
795 hydrothermal vent shrimp species (Alvinocarididae) in the Okinawa Trough, Northwest
796 Pacific. *Mar Ecol Prog Ser* 529:159–169. doi: 10.3354/meps11267

797 Zbinden M, Cambon-Bonavita M (2020) Biology and ecology of *Rimicaris exoculata*, a symbiotic
798 shrimp from deep-sea hydrothermal vents. *Mar Ecol Prog Ser* 652:187–222. doi:
799 10.3354/meps13467

800 Zhou Y, Chen C, Zhang D, Wang Y, Kayama H, Jin W, Dass S, Ruiyan B, Han Y, Sun D, Xu P, Lu B,
801 Zhai H, Han X, Tao C, Qiu Z, Sun Y, Liu Z, Qiu W, Wang C (2022) Delineating biogeographic
802 regions in Indian Ocean deep-sea vents and implications for conservation. *Divers Distrib*
803 1–13. doi: 10.1111/ddi.13535

804

Figure 1.

[Click here to access/download;Figure;Figure 1. Sampling fields off Japan.tif](#)

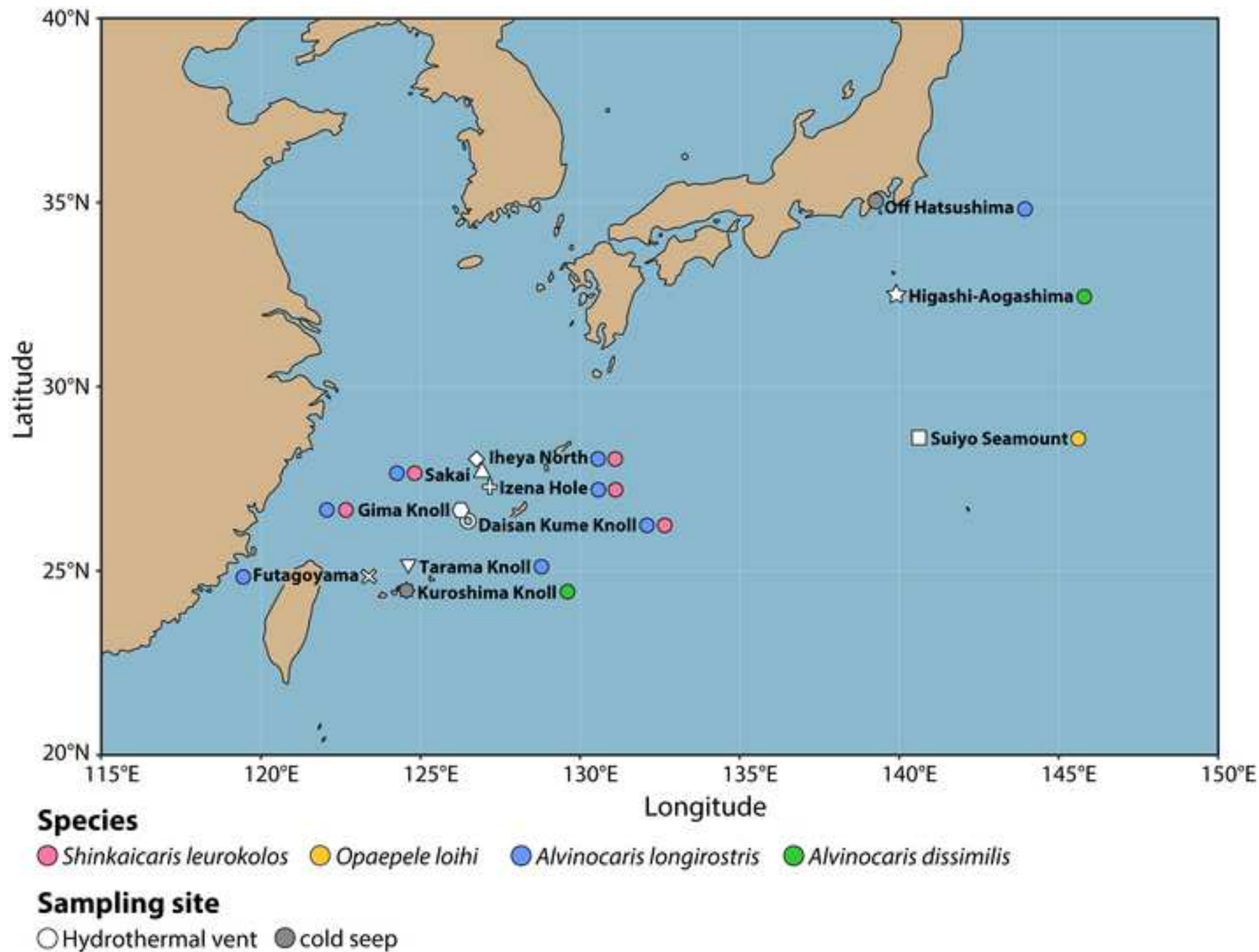


Figure 2.

[Click here to access/download;Figure;Figure 2. Population structure of Alvinocaridids off Japan.tif](#)

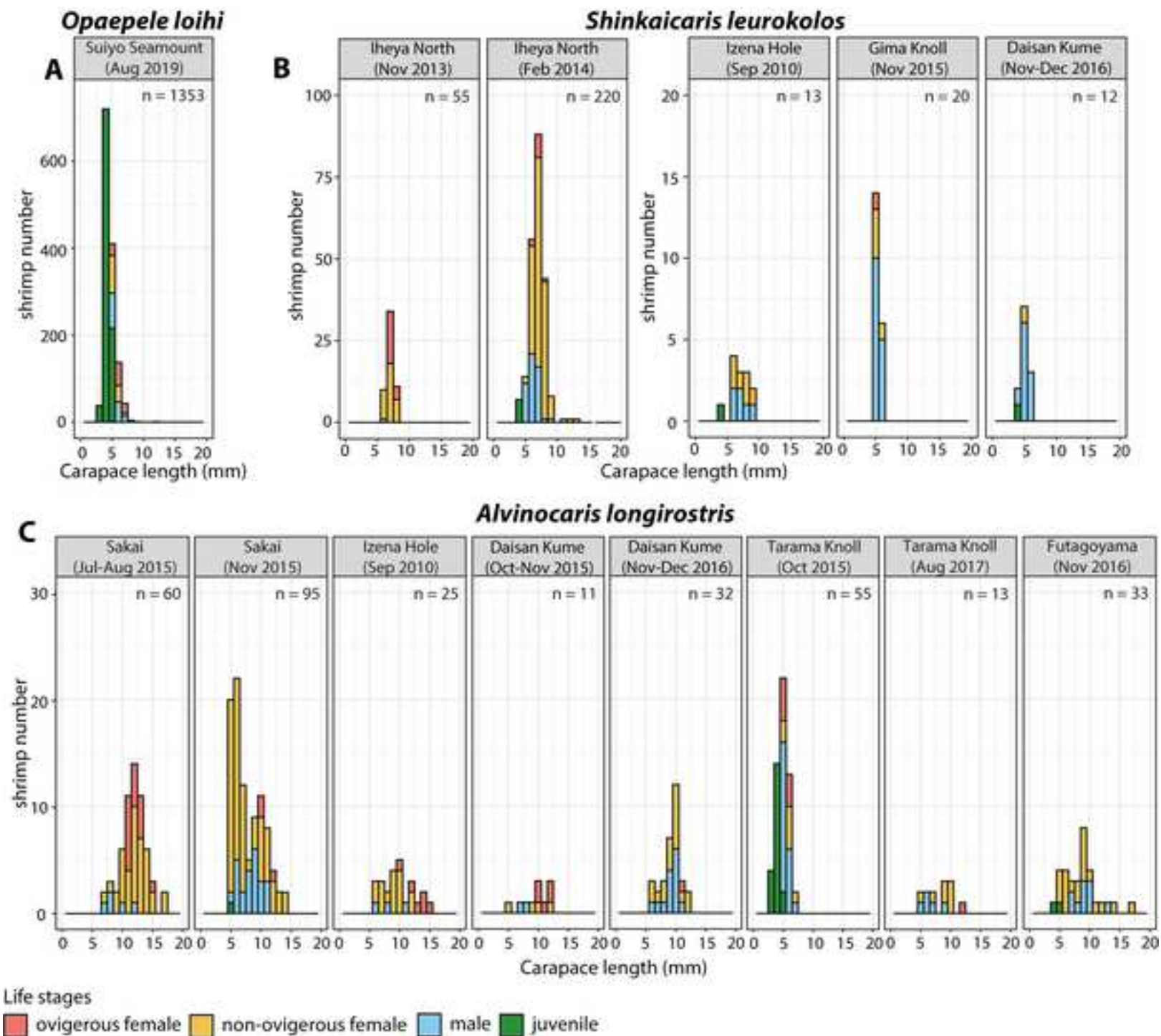


Figure 4.

[Click here to access/download;Figure;Figure 4. Reproductive features of Alvinocaridids off Japan.tif](#)

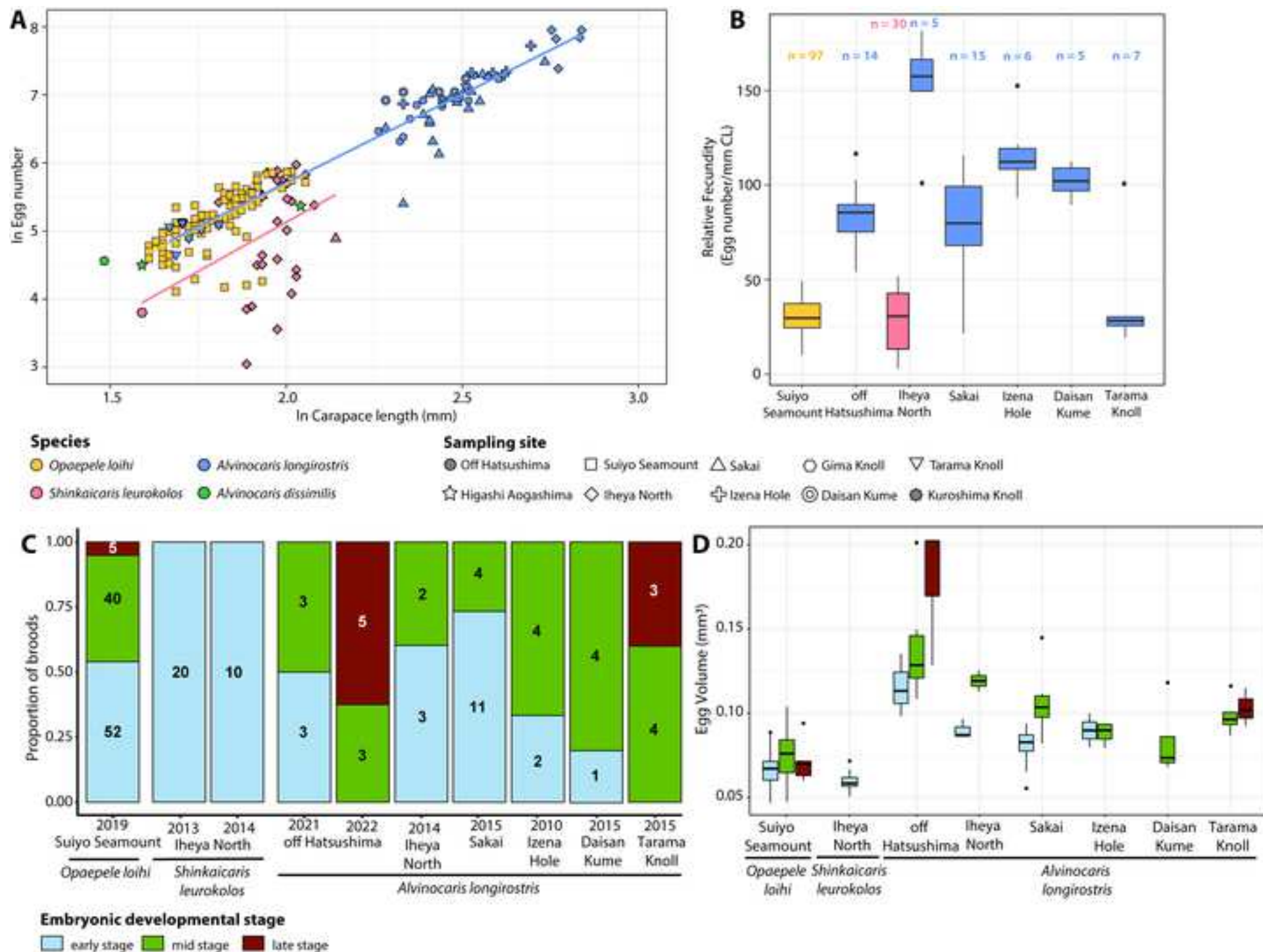


Figure 5.

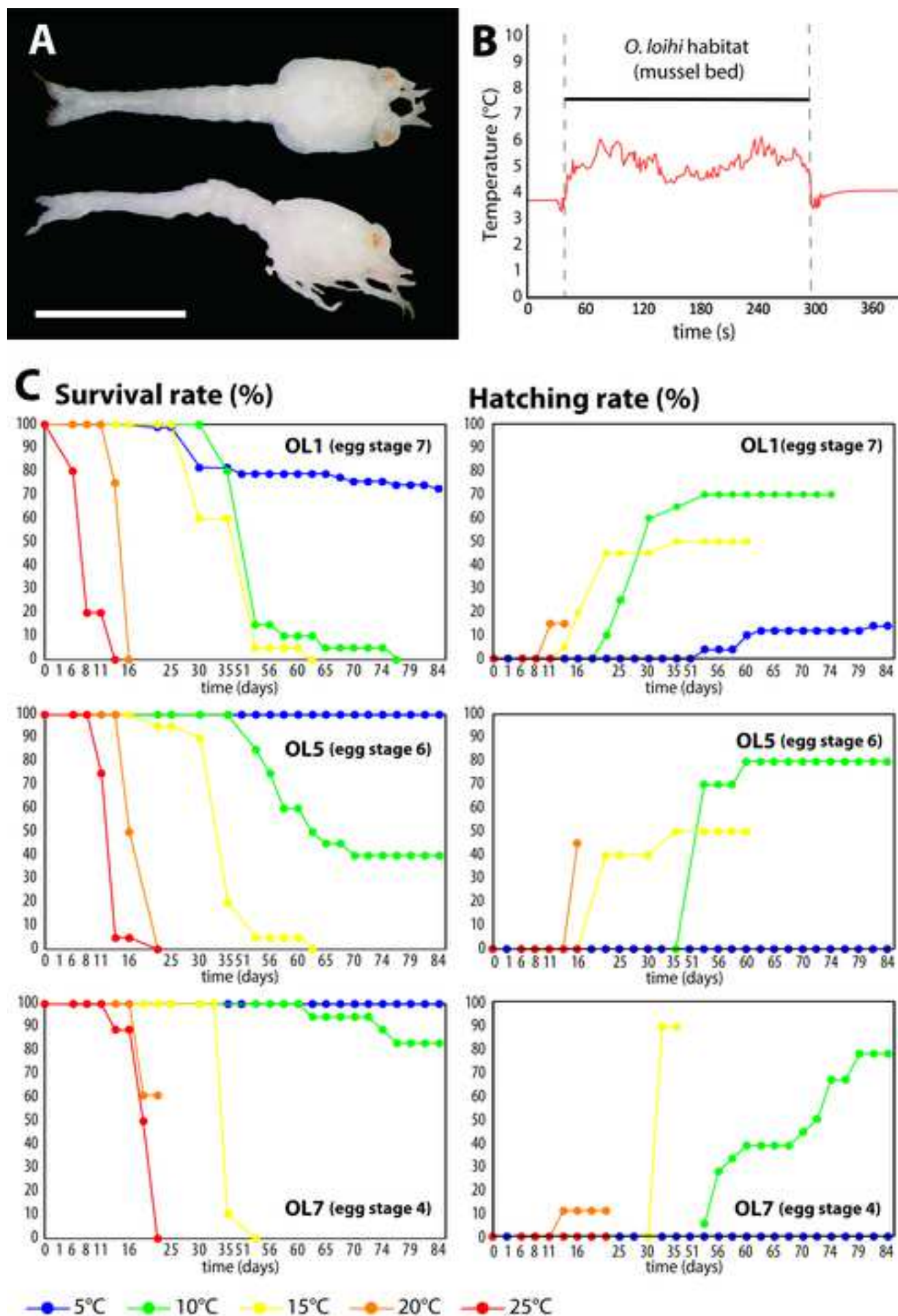


Figure 6.

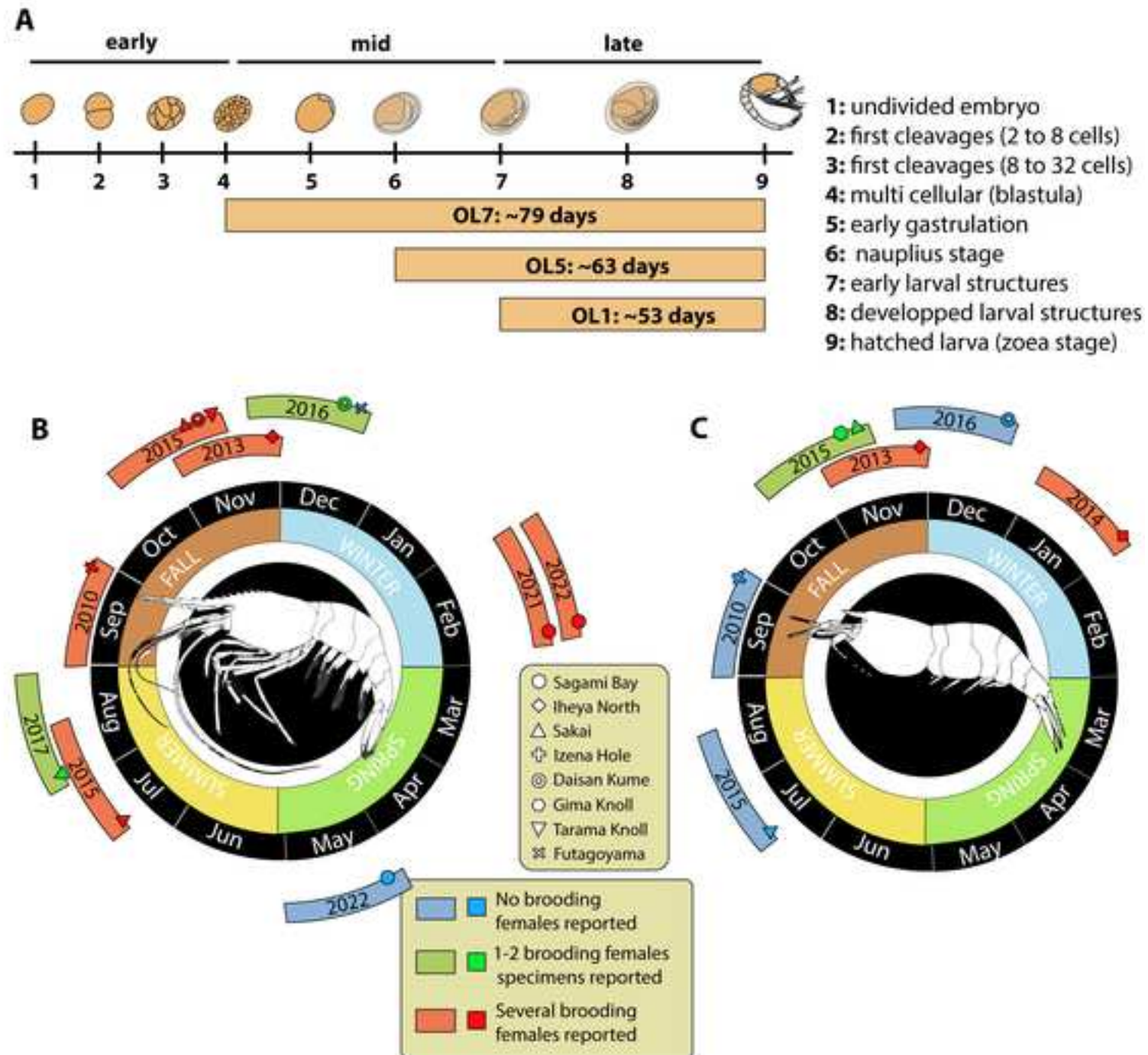


Table 1.

Species	Sampling site (Time period)	Ovigerous female				Female		
		n	mean	max	min	n	mean	max
<i>Opaepele loihi</i>	Suiyo Seamount (Aug 2019)	103	6.04	7.8	5.0	132	5.41	7.4
<i>Shinkaicaris leurokolos</i>	Iheya North (Nov 2013)	20	7.18	8.0	6.6	34	7.03	8.5
	Iheya North (Feb 2014)	10	6.95	7.8	5.6	151	7.28	12.6
	Izena Hole (Sep 2010)	0	-	-	-	6	7.42	8.6
	Gima Knoll (Nov 2015)	0	-	-	-	1	-	5.2
	Daisan Kume (Nov-Dec 2016)	1	-	4.9	4.9	4	5.18	5.6
<i>Alvinocaris longirostris</i>	Sakai (Jul-Aug 2015)	16	12.2	15.4	10.9	39	12.1	16.9
	Sakai (Nov 2015)	3	10.7	12.0	9.8	67	7.56	13.9
	Izena Hole (Sep 2010)	6	13.06	14.8	10.3	16	8.84	12.4
	Daisan Kume (Oct-Nov 2015)	5	11.1	12.3	9.8	4	9.35	12.5
	Daisan Kume (Nov-Dec 2016)	1	-	11.5	11.5	17	9.32	12.0
	Tarama Knoll (Oct 2015)	7	5.6	6.1	5.3	7	5.8	6.6
	Tarama Knoll (Aug 2017)	1	-	12.3	-	7	8.56	10.1
	Futagoyama (Nov 2016)	0	-	-	-	21	9.19	20.7

	Male				Juvenile				Sex ratio		
min	n	mean	max	min	n	mean	max	min	M:F	χ^2	p
4.9	145	5.72	12.1	4.9	973	4.24	4.8	3.2	0.62	22.94	***
5.9	1	-	6.1	6.1	0	-	-	-	0.02	51.07	***
4.6	52	6.29	8.8	4.8	7	4.1	4.4	3.6	0.32	55.78	***
6.0	6	7.3	9.0	6.0	1	-	4.2	4.2	1.0	0	NS
5.2	11	5.24	6.2	4.5	1	-	4.0	4.0	11.0	8.33	**
4.8	15	5.33	5.9	4.6	0	-	-	-	3.0	5	*
7.1	5	8.8	11.9	6.9	0	-	-	-	0.09	41.67	***
4.8	24	8.34	10.8	5.5	1	-	4.7	4.7	0.34	22.51	***
6.1	3	8.4	11.2	5.8	0	-	-	-	0.14	14.44	***
5.4	2	7.35	7.8	6.9	0	-	-	-	0.22	4.45	*
6.4	14	9.09	10.6	6.4	0	-	-	-	0.78	0.5	NS
4.9	21	5.44	7.4	4.8	20	3.84	4.6	3.1	1.5	1.4	NS
5.0	5	6.7	9	4.8	0	-	-	-	0.63	0.69	NS
4.9	10	9.26	13.0	6.6	2	4.6	4.7	4.5	0.48	3.9	NS

Table 2.

Species	Sampling site	Sampling period	Cohort 1			Cohort 2	
			%	μ	σ	%	μ
<i>Opaepele loihi</i>	Suiyo Seamount	August 2019	72.9	4.3	0.4	27.1	5.5
<i>Shinkaicaris leurokolos</i>	Iheya North	November 2013	100	7.1	0.5	-	-
		February 2014	13.8	5.2	0.8	84.8	7.1
<i>Alvinocaris longirostris</i>	Sakai	July-August 2015	6.0	7.3	0.4	94.0	12.1
		November 2015	52.3	5.8	0.7	47.6	10.0
	Tarama Knoll	October 2015	100	4.8	1.0	-	-

Cohort 3			
σ	%	μ	σ
0.9	-	-	-
-	-	-	-
0.7	1.4	12.0	0.02
1.8	-	-	-
1.7	-	-	-
-	-	-	-

Table 3.

				<i>Shink</i>		
Sampling site	Assemblage number	Assemblage type	Sampling year	OvF	F	M
Iheya North - Original	Assemblage_1	Chimney rocks	November 2013	20	34	1
Iheya North - Original	Assemblage_1	<i>Shinkaia</i> aggregation	February 2014	0	1	3
Iheya North - Original	Assemblage_2	Chimney rocks	February 2014	2	51	5
Iheya North - Original	Assemblage_3	Chimney rocks	February 2014	7	81	10
Iheya North - Original	Assemblage_4	Chimney rocks	February 2014	0	0	18
Iheya North - Original	Assemblage_5	Chimney rocks	February 2014	1	5	15
Sakai - Hitoshi	Assemblage_1	<i>Shinkaia</i> aggregation	July 2015	0	5	1
Sakai - Hitoshi	Assemblage_2	Mussel bed	July 2015			
Sakai - Noho	Assemblage_3	<i>Shinkaia</i> aggregation	August 2015			
Sakai - Noho	Assemblage_4	<i>Shinkaia</i> aggregation	August 2015			
Sakai - Noho	Assemblage_7	Mussel bed	November 2015	1	1	3
Sakai - Noho	Assemblage_8	<i>Shinkaia</i> aggregation	November 2015	1	0	2

<i>aicaris leurokolos</i>					<i>Alvinocaris longirostris</i>							
J	n	M:F	χ^2	p	OvF	F	M	J	n	M:F	χ^2	p
0	55	0.02	15.62	***								
0	4	-	-	-	5	0	0	0	5	-	-	-
0	58	0.09	14.92	***								
0	98	0.11	62.08	***								
2	20	-	18	***								
5	26	2.5	3.86	*								
1	7	-	-	-	4	4	1	0	9	0.13	5.44	*
					7	10	1	0	18	0.06	14.22	***
					2	7	3	0	12	0.33	3	NS
					3	18	0	0	21	0	21	***
0	5	-	-	-	2	34	11	1	48	0.31	13.29	***
0	3	-	-	-	1	33	13	0	47	0.38	9.38	***